INTERNATIONAL
Agrophysics
www.international-agrophysics.org

Int. Agrophys., 2025, 39, 319-330
doi: 10.31545/intagr/202892

Development of pedotransfer functions to predict water-stable aggregates in heated and unheated soils**

Carolina V. Giraldo[1], *Carlos A. Bonilla*[2,3]*

[1]Pontificia Departamento de Ingeniería Hidráulica y Ambiental, Pontificia Universidad Católica de Chile, Av. Vicuña Mackenna 4860, Macul, Santiago, Chile
[2]Department of Crop and Soil Science, Oregon State University, 109 Crop Science Building, Corvallis, OR 97331-3002, United States
[3]Hermiston Agricultural Research and Extension Center, Oregon State University, 2121 S 1st St, Hermiston, OR 97838, United States

Received January 30, 2024; accepted March 12, 2025

Abstract. The wildfire temperature can affect many soil properties, such as aggregate stability. The water stable aggregate (WSA) is a soil property not typically considered in soil analysis, so pedotransfer functions are an alternative for estimating it. This study provides a series of pedotransfer functions as models to predict the effect of heating on WSA using basic soil data. Soil samples were collected from 22 different sites and analyzed in the laboratory before and after being heated at 100 and 300°C. These temperatures represent low- and medium-severity wildfires. Bulk density, organic matter (OM), sand, silt, and clay contents, and pH were used to estimate WSA for unheated and heated soils. The results showed no significant differences in WSA between unheated soils and those heated at 100°C but a significant decrease at 300°C. WSA correlated significantly with OM content and pH in unheated soils and 100°C heated soils ($p<0.01$), but not at 300°C. A non-linear model was developed to predict WSA in unheated soils, and two additional models were developed for heated soils. Finally, at 300°C, the organic matter, clay content, and water-stable aggregates decreased significantly while pH increased.

Keywords: bulk density, organic matter, pedotransfer functions, water-stable aggregates, wildfires

1. INTRODUCTION

Wildfires occur regularly in ecosystems worldwide, and they are the leading cause of changes in natural ecosystems, increasing the risk of soil erosion and redistribution. These events, primarily caused by human activities, lead to soil degradation and nutrient loss through volatilization and erosion (Farid *et al.*, 2024). The effects on soils caused by fire primarily depend on fire intensity, duration, frequency, fuel load, and soil properties (Chicco *et al.*, 2023). Fire intensity is classified according to the temperature reached as low (below 100°C), medium (up to 250°C), and high (over 350°C) (Dhungana *et al.*, 2024). However, the severity mainly depends on fuel load, soil type, moisture content, and fire intensity (Agbeshie *et al.*, 2022). Wildfires can affect physical, chemical, and biological soil properties (Carkovic *et al.*, 2015; Farid *et al.*, 2024; Köster *et al.*, 2021). Fire significantly alters soil chemical properties by reducing nutrient retention, nutrient content, and organic matter while affecting soil fertility, pH, and electrical conductivity (Ayoubi *et al.*, 2021). Additionally, fire weakens soil structure, increases erodibility, and can lead to changes in soil texture. Fire changes in soil physical and chemical properties are often associated with more crumbly, less cohesive, and more erodible conditions. This is mainly due to the combustion of organic matter, which reduces aggregate stability (Chicco *et al.*, 2023). Soil organic carbon is physically protected through its bonds with primary soil particles within aggregates, and these bonds can also enhance aggregate stability (Ayoubi *et al.*, 2020). Then,

*Corresponding author e-mail: carlos.bonilla@oregonstate.edu
**This research was supported by funding from the National Agency for Research and Development, Chile, grant ANID/FONDECYT/REGULAR 1191166 and 1220777.

when aggregates are destroyed, organic matter stores become unprotected, reducing soil structure stability and accelerating soil erosion, especially in hilly regions.

Soil aggregate stability may increase, decrease, or remain unchanged as a result of fire or laboratory heating, depending on the influence of rising temperature on binding agents (Negri *et al.*, 2024). The aggregate stability usually increases in soils with high clay content depending on fire severity (Mataix-Solera *et al.*, 2011), so the higher the fire severity, the higher the aggregate stability (Albalasmeh *et al.*, 2013). Despite this condition, different studies have found that high-intensity fires can increase or decrease the stability depending on the combustion of the organic matter (OM), microbial secretion, or the recrystallization of clay particles (Bai *et al.*, 2020; Hrelja *et al.*, 2020). Thus, some studies have reported no significant changes at 100°C in laboratory experiments (Zavala *et al.*, 2010; Ibrahimi *et al.*, 2019). However, Jiménez-Pinilla *et al.* (2016) found an increase in aggregate stability at 300°C despite the decrease in OM content. Contrary to these findings, Martínez *et al.* (2022) and Giraldo *et al.* (2024) showed a decrease in water-stable aggregates (WSA) at 300°C.

Usually, measuring the changes in soil properties after a wildfire is challenging. There is limited access or restrictions to reach the affected area, and the sampling needs to be done as soon as possible to avoid the effect of other factors, such as wind and water erosion (Bonilla *et al.*, 2014). For that reason, laboratory experiments have been used to simulate wildfire conditions (Li *et al.*, 2022), controlling some of the variables to differentiate the effects of heating (Zhang *et al.*, 2018). It also allows sampling and analyzing immediately after heating (Badía-Villas *et al.*, 2014).

Furthermore, even though aggregate stability is an indicator of soil health due to its relation with soil erodibility and improved soil-water dynamics (Rieke *et al.*, 2022), there is no standard measurement methodology to measure the effect of heating on aggregate stability (Thomaz, 2021). Also, some of the methods can be time-consuming and expensive, making them rarely included in soil analysis routines (Mataix-Solera *et al.*, 2011). Because of this and the previously described sampling and measuring limitations, an alternative option is using pedotransfer functions (PTFs) and machine learning techniques to create useful models to predict aggregate stability (Rivera and Bonilla, 2020). Although aggregate stability prediction using pedotransfer functions has been used in unheated soils, there are not enough studies or models after heating conditions. These functions could assist post-fire assessments where direct measurements are not feasible. Therefore, we selected 22 soils in Central Chile from diverse sites with different conditions to ensure a wide range of soil properties. In this context, the main objective of this study was to create models based on variables usually measured in soil analysis routines or predicting the effect of heating at 100 and 300°C on soil aggregate stability.

2. MATERIALS AND METHODS

2.1. Soil sampling sites

Different locations in Central Chile were selected as sampling sites. These areas consist of a geological depression that extends for about 1000 km from Valparaíso to La Araucanía from 32°S to 42°S (Bonilla and Johnson, 2012). Average annual rainfall ranges from 270 mm in northern Central Chile to 1 150 mm in the southern areas. The temperature in this region follows a seasonal pattern, with cold winters (minimum 0°C) and hot summers (maximum 28°C). In general, sites near the mountains experience greater daily temperature variation, while coastal locations have more stable temperatures throughout the day (Contreras and Bonilla, 2018). The Köppen-Geiger classification of the study area includes Mediterranean (Csb) and Marine West Coast (Cfb) climates (Sarricolea *et al.*, 2017). According to the Natural Resources Information Center (1996a, 1996b, 1997a, 1997b, 2002), most soils between the Valparaíso and Maule regions are sedimentary, primarily formed from alluvial deposits. In contrast, the soils of La Araucanía predominantly consist of volcanic ash deposits. Thus, clay minerals of some soils of the first group of regions include montmorillonite (Molina-Roco *et al.*, 2018), while volcanic soils of the south of Central Chile contain allophane and imogolite (Valle *et al.*, 2018). Central Chile was selected as the study area due to its records as the area with the highest number of fire events (92%) and burnt surface areas (89%) in the country from 1964 to 2022 (Corporación Nacional Forestal., 2024; Giraldo *et al.*, 2024).

2.2. Soil sampling

Twenty-two sites were selected for collecting soil samples between 2017 and 2022 (Fig. 1). Sixteen of those samples were described previously in Giraldo *et al.* (2024). Soil types included Alfisols, Inceptisols, Mollisols, Andisols, Entisols and Ultisols. These soils were predominantly loamy or sandy loam texture classes, with OM contents between 1.57 and 21.53%. Samples were collected from topsoil (0-15 cm depth) using plastic bags, then, they were air-dried, and sieved using a 2-mm sieve in the laboratory. Soil samples were divided into three aliquots for heating treatments. Sieved soil samples were heated at 100 and 300°C. We selected these temperatures because they can simulate low and medium-severity burns which are common in wildfires in Mediterranean-type ecosystems (Marcos *et al.*, 2018) such as Central Chile. In addition, 100°C treatment because at these temperatures the soil dehydrates without significantly altering the properties (Aedo and Bonilla, 2021). In contrast, at 300°C, the organic matter and the soil structure are significantly affected (Terefe *et al.*, 2008). These temperatures were also selected because, according to Marcos *et al.* (2007), heating soils at low temperatures (100°C) at long exposure times produces similar

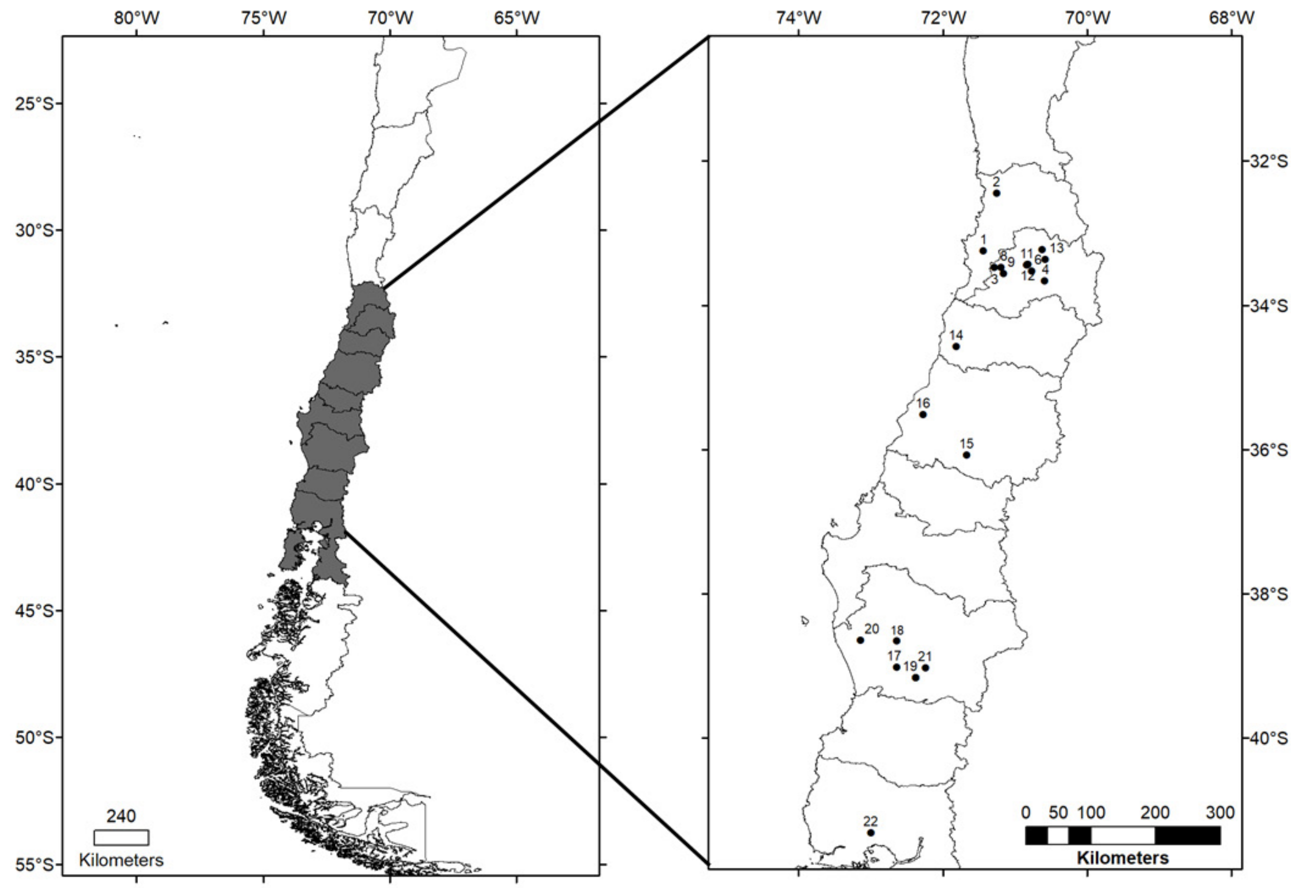

Fig. 1. Sampling locations employed in this study. The map represents the administrative division from Valparaíso to Los Lagos.

effects to high temperatures. To heat the soil samples to 300°C, three 250 mL ceramic containers were placed into a muffle for two hours, according to Martínez *et al.* (2022).

2.3. Soil properties measurements

The water-stable aggregates (WSA) were measured in triplicates by using a wet sieving apparatus (Royal Eijkelkamp, 2022) according to Kemper and Rosenau method (1986). Four grams of air-dried 1-2 mm aggregates were wet sieved using a 0.25 mm sieve immersed in distilled water for 3 min. The unstable aggregates passed through the sieve and were collected in the distilled water-filled can underneath the sieve. The process was repeated with a dispersing solution, either sodium hexametaphosphate (2 g L^{-1}) for pH > 7.0 or sodium hydroxide (2 g L^{-1}) for pH < 7.0 for 8 min. The collected cans, with water or dispersing solution, were dried at 110°C until the water was evaporated. The WSA is calculated as the percentage of stable aggregates, calculated by dividing the weight of the stable aggregates obtained from the dispersing solution containers by the total weight of both stable and unstable aggregates. A 100% value indicates no breakage, and 0% states a complete aggregate breakage (Rivera and Bonilla, 2020).

In addition, the bulk density, OM content, pH, and soil texture were also measured in triplicates. The bulk density was measured using the 3B USDA method, which used 250 cm^3 stainless steel cylinders (Soil Survey Staff, 2022). The OM was measured using the Walkley-Black method (Walkley and Black, 1934). The pH was measured using deionized water with a 1:2.5 soil-to-solution ratio, with measurements taken from the supernatant. Soil texture was determined using a PARIO device software version 1.0.4.0 (METER Group, Inc, Pullman, WA, USA) as described by Acevedo *et al.* (2021). For each sample, three duplicate beakers were prepared: The first and second beakers were treated with 100 mL of sodium hexametaphosphate (50 g L^{-1}) and 250 mL of distilled water, then shaken overnight to ensure proper dispersion. The third beaker was placed in an oven at 105°C and weighed to determine organic matter loss and accurately measure the solid mass. The dispersed solutions were transferred to a standard 1-L sedimentation cylinder and agitated for 1 min to initiate the measurement. Results were recorded at 8 h and 60 s, following the approach described by Durner *et al.* (2017).

2.4. Data analysis and statistics

The analysis included: a) the descriptive analysis of how soil properties are affected by heat, b) the correlations between WSA and other soil properties, and c) the use of models to estimate WSA affected by heating. The descriptive statistics were computed using the R Software, version 4.2.2 (R Core Team, 2022), tidyverse, version 1.3.2. (Wickham *et al.*, 2019) and ggplot2, version 3.4.0 (Wickham, 2016).The descriptive analysis included the Wilcox test in determining if there were significant differences between unheated soils and soils heated at 100 and 300°C. Correlations were calculated using the R package complot, version 0.95 (Wei and Simko, 2024). In addition, the generalized reduced gradient (GRG) was used in Excel with Solver to fit the models. The GRG method is more parsimonious and easily interpretable because it uses fewer parameters (Archontoulis and Miguez, 2015). In addition, nonlinear models were used to compare the model proposed by Rivera and Bonilla (2020) and a proposed model for unheated soils. To estimate WSA at 100 and 300°C, we developed two types of models: The first one with only measured soil properties, including WSA in unheated soils, and the second with measured soil properties and predicted WSA using the most accurate model for unheated soils. The explanatory variables of the unheated WSA model were bulk density (BD), soil texture, OM content, and pH, while the output was the WSA. In heated conditions, the explanatory variables included also measured WSA or predicted WSA in unheated conditions.In addition, the generalized reduced gradient (GRG) was used in Excel with Solver to fit the models. The GRG method is more parsimonious and easily interpretable because it uses fewer parameters (Archontoulis and Miguez, 2015). In addition, nonlinear models were used to compare with the model proposed by (Rivera and Bonilla, 2020). Using measured data and predicted data, WSA at 100 and 300°C were estimated based on soil properties in unheated soils in two different models. The explanatory variables were bulk density (BD), soil texture, OM content, and pH, while the output was the WSA. Although properties such as the CEC, EC, and cations could be relevant, their measurement can be expensive and time-consuming (Khaledian *et al.*, 2017; Rivera and Bonilla, 2020). To evaluate the fitting between measurements and estimates, we used the coefficient of determination (R^2), and the root mean square error (RMSE) by using the following equation:

$$RMSE = \sqrt{\frac{\sum_{i=1}^{n}(P_i - O_i)^2}{n}},$$

where: O_i corresponds to the observed data, P_i corresponds to the model prediction data, and n is the number of observations.

3. RESULTS AND DISCUSSION

3.1. Heating effect on chemical and physical properties

The average and the standard deviation of the measured variables of this study, categorized by temperature, are shown in Table 1. Unheated soil samples showed an average bulk density of 1.15 g cm^{-3}, linked to the predominantly loamy or sandy loam texture classes. Soils also showed OM contents between 1.6 and 21.5%. The samples' WSA was around 65%, indicating that 35% of the aggregates are easily destroyed in water. The medium value for stability is explained by the fact that half of the soil samples had OM contents below 5%, and more stable aggregates are found with larger OM contents (Topa *et al.*, 2021).

When heated at 100°C, the chemical and physical soil properties did not differ from the unheated soils. This condition was reported in previous studies by Inbar *et al.* (2014), Ye-Yang Chun *et al.* (2021), and Martínez *et al.* (2022). Shrublands and open vegetation characterize central Chile (Meserve *et al.*, 2020). Under fire conditions, the limited availability of fuel in these types of ecosystems and vegetation leads to low-severity burn (Stavi, 2019), with temperatures similar to 100°C (Marcos *et al.*, 2018). At 300°C, clay significantly decreased ($p<0.001$), from 19% in unheated soils to 10% after burning. These results are like those reported by Inbar *et al.* (2014), in which the decrease in clay was attributed to the aggregation of clay particles into larger particles resembling silt or sand. In addition, the OM content decreased significantly ($p<0.001$), from 8.83% in unheated soils to 2.95% after heating. These results agree with previous studies conducted by Negri *et al.* (2021), Martínez *et al.* (2022), Acevedo *et al.* (2023), and Giraldo *et al.* (2024). The WSA significantly decreased ($p<0.05$) from 74% in unheated soils to 62% at 300°C. This means that 26% of aggregates broke apart quickly in water when soils were unheated but increased to 38% when the soils were heated at 300°C. These results were expected and can be attributed to the oxidation of the OM that leads to the disaggregation of the soil structure and macropores breakdown (Agbeshie *et al.*, 2022). According to Fox *et al.* (2007), when the OM content decreases, the WSA decreases, showing a correlation between them (Ayoubi *et al.,* 2021; Martínez *et al.*, 2022). Fires contribute to soil aggregate breakdown, affecting soil structure, health, and quality by reducing porosity and degrading soil functions (Roshan and Biswas, 2023). The pH significantly increased ($p<0.001$) from 6.53 to 7.41, attributed to the denaturalization of organic acids (Chicco *et al.*, 2023). These results are like those reported by Terefe *et al.* (2008) and Martínez *et al.* (2022).

Table 1. Main properties of the soil samples based on heating temperature

Site	Lat. S	Long. W	Texture	Heat temperature	Bulk density (g cm^{-3})	Sand	Silt	Clay	Organic matter	pH	Water stable aggregates (%)
						(%)					
1	33°15'	71°26'	Loam	Unheated	1.14	51	34	15	7.87	5.85	97
			Sandy loam	100°C	-	55	29	16	8.40	6.09	94
			Loam	300°C	-	51	37	12	1.67	7.60	55
2	32°27'	71°15'	Sandy clay loam	Unheated	1.67	61	18	21	2.10	7.02	36
			Sandy clay loam	100°C	-	59	21	20	1.73	7.12	32
			Sandy loam	300°C	-	64	20	16	0.73	7.39	70
3	33°28'	71°16'	Sandy loam	Unheated	1.79	67	16	17	3.40	5.89	87
			Sandy loam	100°C	-	69	16	15	3.20	6.27	87
			Sandy loam	300°C	-	69	13	18	1.33	6.81	92
4	33°40'	70°35'	Loam	Unheated	1.12	48	40	12	1.57	8.13	25
			Loam	100°C	-	49	42	9	1.30	7.97	40
			Sandy loam	300°C	-	53	41	7	0.39	7.84	59
5	33°27'	70°50'	Loam	Unheated	1.07	46	38	16	4.57	6.91	55
			Loam	100°C	-	45	43	12	4.10	7.38	20
			Loam	300°C	-	48	45	7	1.70	8.44	23
6	33°31'	70°45'	Loam	Unheated	1.30	50	30	20	4.97	7.94	78
			Sandy loam	100°C	-	56	33	11	4.77	8.18	48
			Sandy loam	300°C	-	58	37	6	2.00	8.88	24
7	33°26'	70°49'	Clay loam	Unheated	1.28	21	43	36	3.83	6.99	72
			Clay loam	100°C	-	21	41	38	3.83	6.64	57
			Silt Loam	300°C	-	26	55	19	1.10	7.75	43
8	33°29'	71°11'	Sandy loam	Unheated	1.22	63	24	13	12.80	6.40	86
			Sandy loam	100°C	-	58	28	14	10.83	6.26	79
			Sandy loam	300°C	-	63	29	8	4.70	9.07	81
9	33°34'	71°9'	Silty clay	Unheated	1.33	13	47	40	4.53	8.29	75
			Silty clay loam	100°C	-	19	44	37	5.13	7.69	56
			Loam	300°C	-	37	43	20	1.17	7.97	100
10	33°14'	70°37'	Sandy loam	Unheated	1.23	63	24	13	5.50	7.47	52
			Sandy loam	100°C	-	61	23	16	4.43	7.09	35
			Sandy loam	300°C	-	64	32	4	2.00	7.75	69
11	33°27'	70°50'	Loam	Unheated	1.34	50	33	17	2.10	7.49	53
			Loam	100°C	-	52	32	16	2.37	7.35	59
			Sandy loam	300°C	-	54	37	9	0.98	7.85	61
12	33°26'	70°49'	Loam	Unheated	1.19	40	46	14	1.63	6.55	73
			Loam	100°C	-	42	42	16	1.70	6.47	76
			Loam	300°C	-	44	48	8	0.42	7.38	68
13	33°26'	70°49'	Silt loam	Unheated	0.84	18	63	19	12.97	6.51	86
			Silt loam	100°C	-	19	56	25	13.10	6.24	55
			Silt loam	300°C	-	23	66	11	4.33	8.36	28

Table 1. Continuation

Site	Lat. S	Long. W	Texture	Heat temperature	Bulk density (g cm^{-3})	Sand	Silt	Clay	Organic matter	pH	Water stable aggregates (%)
						(%)					
14	34°34’	71°48’	Loam	Unheated	1.27	51	31	18	3.43	6.01	74
			Sandy clay loam	100°C	-	52	28	21	3.50	6.12	63
			Loam	300°C	-	51	31	18	2.23	7.18	41
15	36°4’	71°39’	Loam	Unheated	1.26	47	43	10	8.17	5.83	72
			Sandy loam	100°C	-	57	34	9	7.60	5.83	43
			Sandy loam	300°C	-	61	37	2	3.27	5.67	61
16	35°31’	72°16’	Silt loam	Unheated	0.88	21	62	17	13.23	5.22	78
			Silt loam	100°C	-	30	63	7	15.83	5.00	74
			Silt loam	300°C	-	34	64	2	6.77	6.25	75
17	38°39’	73°7’	Silt loam	Unheated	0.68	35	54	11	20.97	5.46	95
			Loam	100°C	-	40	46	14	19.40	5.65	85
			Silt loam	300°C	-	36	51	13	3.97	6.54	84
18	38°39’	72°37’	Silty clay loam	Unheated	1.18	16	47	37	12.03	5.30	96
			Silty clay	100°C	-	16	43	41	12.37	5.59	87
			Silt loam	300°C	-	22	67	11	3.73	6.85	88
19	39°1’	72°13’	Silt loam	Unheated	0.62	20	59	21	19.27	6.15	97
			Silt loam	100°C	-	35	53	12	19.90	6.33	92
			Silt loam	300°C	-	19	71	10	6.37	8.06	43
20	39°1’	72°37’	Clay loam	Unheated	1.01	23	46	31	13.57	4.94	96
			Loam	100°C	-	27	47	26	13.43	5.55	85
			Silt loam	300°C	-	37	53	10	3.20	6.54	87
21	39°10’	72°22’	Loam	Unheated	0.76	36	45	19	21.53	5.63	83
			Silt loam	100°C	-	37	50	13	18.87	4.89	87
			Sandy loam	300°C	-	52	47	1	8.63	5.91	73
22	41°19’	72°59’	Sandy loam	Unheated	0.69	59	39	2	14.77	6.30	93
			Sandy loam	100°C	-	60	30	10	13.17	6.27	85
			Sandy loam	300°C	-	55	39	6	2.67	7.07	53

Figure 2 shows the relations between selected soil properties before and after heating. Properties such as the clay (Fig. 2a) and the OM (Fig. 2b) contents showed a strong linear relation in the unheated soils and those exposed at 100°C ($R^2 > 0.7$) because low-severity burn conditions do not lead to drastic changes in soil properties. Despite this, the WSA (Fig. 2c) showed a moderate relation ($R^2 = 0.66$) between unheated soils and heated to 100°C, which is attributed to the increment in instability when the aggregates are subjected to heat. In shrublands, temperatures related to low-severity burn may cause a slight decrease in OM and aggregate stability (Stavi, 2019), similar to our results. On the other hand, when heated to 300°C, linear regressions showed weaker relations for the clay content ($R^2 < 0.3$) and no relation for the WSA ($R^2 < 0.02$). However, the OM content still showed a linear relation ($R^2 = 0.75$).

3.2. Relations between WSA and soil properties affected by the heating

Heating conditions affected the WSA and its correlation with other soil properties. Thus, in unheated soils, WSA showed a positive correlation with the OM content ($R^2 = 0.69$, $p = 0.001$) and a negative correlation with pH ($R^2 = -0.66$, $p = 0.001$). At 100°C, the correlations remained almost the same due to the slight change in the soil properties. Correlations between OM content, pH, and WSA were also reported by Ramírez *et al.* (2020) and Rivera

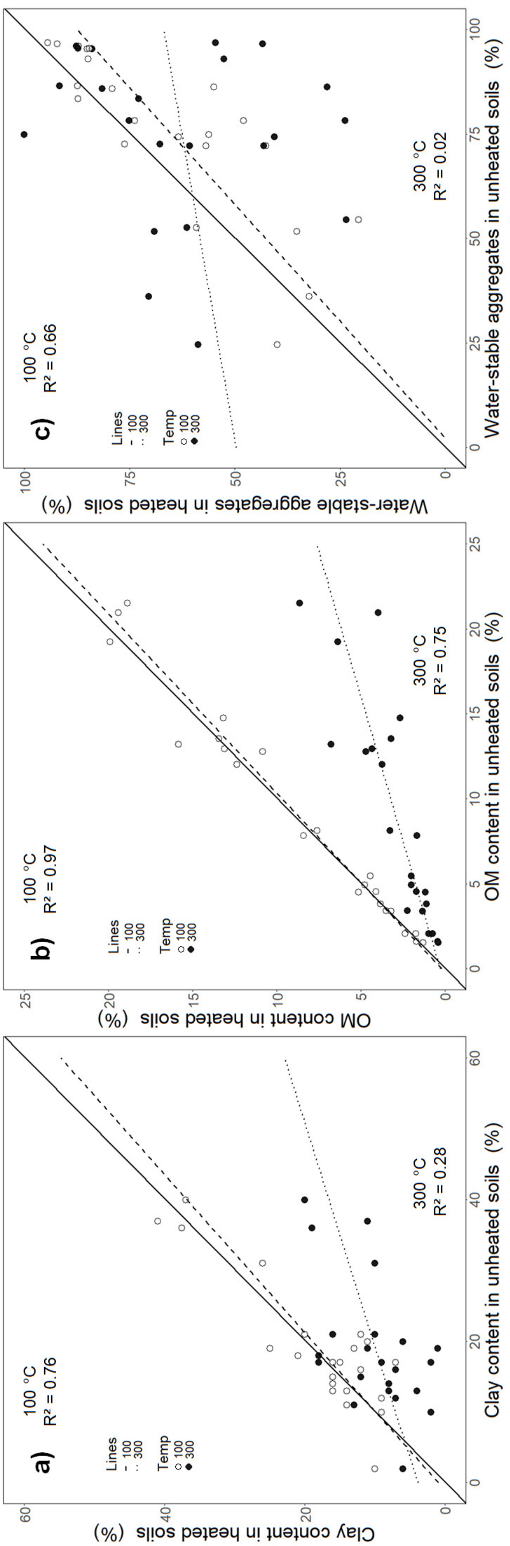

Fig. 2. Relationships between: a) clay, b) organic matter (OM), and c) water-stable aggregates (WSA) in heated and unheated soils. White and black dots represent soils heated at 100 and 300°C, respectively. Lines represent the linear regression between unheated and heated soils at 100°C (dashed) and between unheated and heated soils at 300°C (dotted), respectively. The 1:1 line is shown as a reference (solid line).

and Bonilla (2020). After heating to 300 °C, there were no significant correlations with other soil properties though previous studies reported relevant relationships between OM content and WSA (Fox *et al.*, 2007; Martínez *et al.*, 2022). This condition could be attributed to changes in other soil cementing agents, which may not be related to the OM content. According to Campo *et al.* (2014), these variations in aggregation by heating could respond to variations in soil inorganic compounds or changes in clay fraction.

Table 2 shows the models developed in this study. The table compares the model proposed by Rivera and Bonilla (2020) and a new model (#1) generated for unheated soils using measured values at controlled conditions (Fig. 3a). The relative importance of explanatory variables in non-linear models was calculated using the R package relsimpo (Groemping, 2007). Rivera and Bonilla's model consists of a linear regression based on OM content, clay, and pH designed using machine learning and 109 soil samples. When used to predict the measured values of this study, the R^2 was 0.58 ($p<0.0001$), with an RMSE of 12.91%. The proposed model #1 is a non-linear model based on bulk density, pH, OM, sand, and silt content built on a set of 22 independent samples. This model showed an R^2 of 0.66 ($p<0.0001$) and an RMSE of 11.55%. The variable that showed the highest importance in this model was silt (99%), followed by pH (0.6%). In a study conducted by Ozlu and Arriaga (2021), there was a correlation between silt and 1-2 mm aggregates attributed to the high silt content of those soils. Half of the soil samples in the present study showed more silt than sand. Both models were compared, and the regression between the predicted WSA of both models had an R^2 of 0.92 (Fig. 3b), which implies that both models are equivalent, making model #1 an option to be used to predict WSA in unheated conditions.

The model by Rivera and Bonilla (2020) was not designed to predict soils subjected to heat, so two models for heated soils were developed using unheated basic soil properties (Table 2). The measured WSA values in unheated soils ($WSA_{UH\_measured}$) are used as input in the first model (#2), and the predicted WSA values ($WSA_{UH\_predicted}$) obtained from the proposed model are used in the second model (#3). In this way, the user can select model #2 or #3 depending on the access to measured WSA values.

When predicting the WSA after heating at 100°C, both models (#2 or #3) use sand, silt, clay, OM content, and pH. The regression between the measured WSA at 100°C (Fig. 4a) and the predicted WSA using model #2 had an R^2 of 0.76 ($p<0.001$) with an RMSE of 10.75%. This model tends to overestimate measured values. The variable with the highest importance in model #2 was OM (49%), followed by $WSA_{Unheated\_measured}$ (46%). This was expected due to the correlation between the WSA and the OM content. On the other hand, model #3 showed an R^2 of 0.53 ($p = 0.0001$) with an RMSE of 14.92%. However, this model underestimated the measured values. The variable that

Table 2. Models for predicting WSA using basic soil properties. One model is proposed for unheated soils and two for specific heating temperatures (100 and 300°C)

Temperature	Model	Equation	R^2	RMSE
Unheated	Rivera and Bonilla (2020)	$WSA = 122 + 1.1\ OM + 0.19\ Clay + 9.1\ pH$	0.58	12.91
	#1	$WSA = 376\ BD^{0.03} - 250\ Sand^{0.03} - 333\ Silt^{0.71} + 4073\ OM^{0.003} - 0.01\ pH^{3.59} - 11.46$	0.66	11.15
100°C	#2	$WSA = 6.43\ Sand^{0.34} + 3.26\ Silt^{-0.21} + 2.05\ Clay^{0.47} + 2.93 \times 10^{-7}\ OM^{5.68} - pH^{0.12} + 2.19 \times 10^{-4}\ WSA_{UH\_measured}^{2.74} + 0.08$	0.76	10.76
	#3	$WSA = -13.82\ Sand^{-42.93} + 251.25\ Silt^{-19.56} + 2315\ Clay^{-7.30} + 0.04\ OM^{2.07} + 487\ pH^{-0.82} - 9.70 \times 10^{-7}\ WSA_{UH\_predicted}^{3.51} - 43.43$	0.53	14.92
300°C	#4	$WSA = 1154\ Silt^{-1.21} + 1.07 \times 10^{-9}\ Clay^{6.66} + 1.13 \times 10^{-4}\ OM^{3.90} + 1496\ pH^{-2.10} + 0.46\ WSA_{UH\_measured}^{-1.86} + 0.79$	0.54	14.77
	#5	$WSA = 723\ Silt^{-0.76} + 1.67 \times 10^{-10}\ Clay^{7.19} + 348\ OM^{-4.07} + 87.47\ pH^{-0.34} + 0.45\ WSA_{UH\_predicted}^{31.17} - 114$	0.63	13.22

BD – bulk density (g cm^{-3}), OM – organic matter content (%). $WSA_{UH\_measured}$ – water-stable aggregates measured in unheated (UH) soils, $WSA_{UH\_predicted}$ – water-stable aggregates in unheated soils predicted using the proposed model. Sand, silt, and clay are expressed in %.

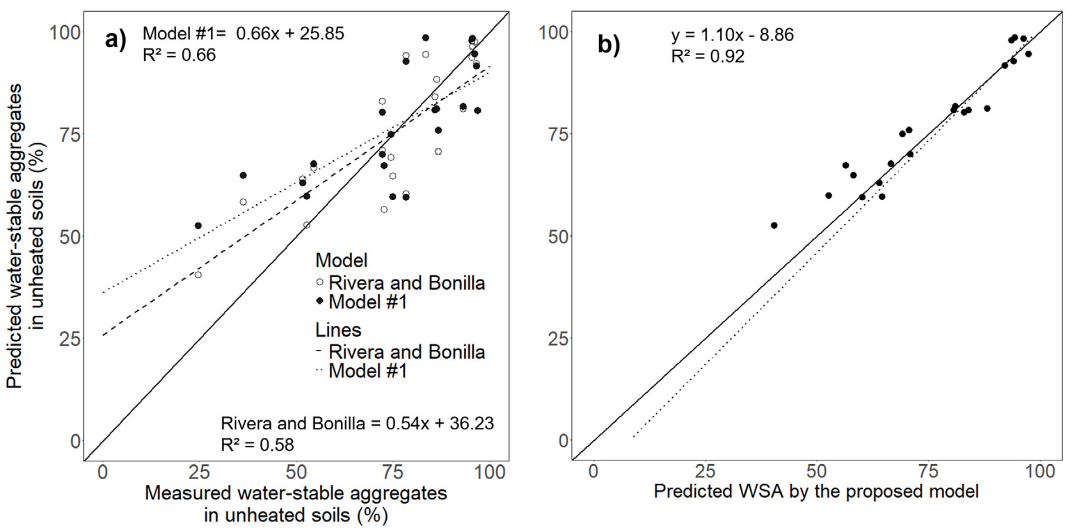

Fig. 3. Comparison between: a) measured and predicted water-stable aggregates (WSA) in unheated soils and b) the data predicted by both models. White dots represent the model proposed by Rivera and Bonilla (2020), and the black dots represent the proposed model #1. Lines represent the linear regression between measured and predicted values by Rivera and Bonilla´s model (dashed) and model #1 (dotted). The 1:1 line is shown as a reference (solid line).

showed the highest importance in model #3 was pH (92%), followed by clay (5%). The interaction between clay, OM, and WSA is affected by pH according to Rivera and Bonilla (2020). In addition, a linear regression between models #2 and #3 showed an R^2 of 0.60, so in the absence of measured data, it is possible to use predicted unheated WSA to have a fair estimate. Traditional methods for measuring aggregate stability are costly and impractical for routine soil surveys (Rivera and Bonilla, 2020). In addition, field campaigns require samplings in both areas affected by wildfires and in adjacent unburnt areas to minimize edge effects (Dhungana *et al.*, 2024), making them time-consuming and expensive (Rieke *et al.*, 2022). However, pedotransfer functions offer a more affordable alternative, allowing for higher sampling (Clergue *et al.*, 2023). As a result, using typical soil properties proved to be useful for creating simple models to predict WSA at 100°C.

When estimating the WSA after heating to 300°C (Fig. 4b), both models (#4 or #5) use silt, clay, OM, and pH and either, measured or predicted unheated WSA values (Fig. 4b). The relation between the measured and predicted WSA values at 300°C using model #4 had an R^2 of 0.54 ($p<0.001$) with an RMSE of 14.77%. The variable that showed the highest importance in model #4 was pH (55%),

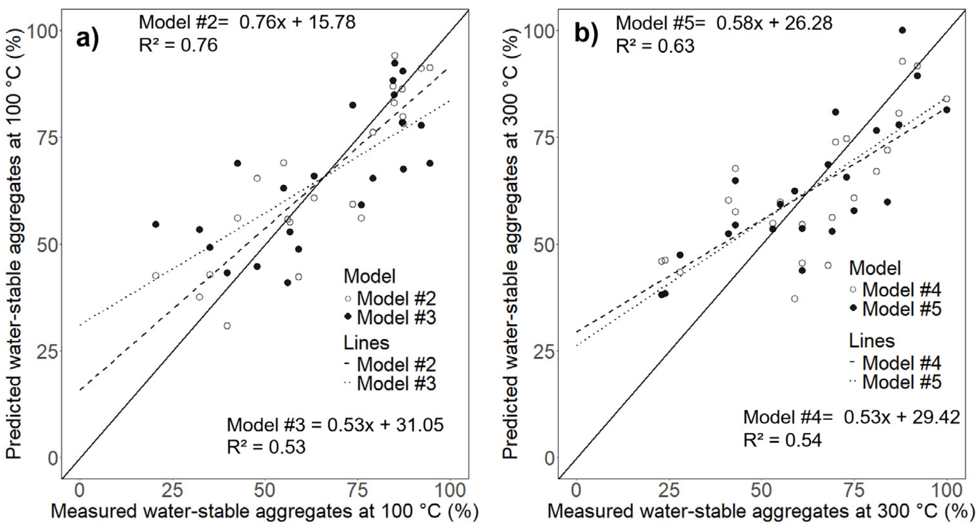

Fig. 4. Comparison between: a) measured and predicted water-stable aggregates (WSA) at 100°C using measured unheated water-stable aggregates (Model #2) and predicted unheated water-stable aggregates (Model #3), and b) measured and predicted water-stable aggregates (WSA) at 300°C using measured unheated water-stable aggregates (Model #4) and predicted unheated water-stable aggregates (Model #5). White dots represent models #2 and #4, and black dots represent models #3 and #5, respectively. Dashed lines show the linear regression between measured and predicted values using models #2 and #4, and dotted lines show the linear regression between measured and predicted values using models #3 and #5, respectively. The 1:1 line is shown as a reference (solid line).

followed by clay (33%). Although the pH showed significant changes at 300°C, it was expected that OM content could show more relevance in the model. Model #5 showed an R^2 of 0.63 ($p<0.001$) with an RMSE of 13.22%. The variable that showed the highest importance in model #5 was clay (83%), followed by silt (14%). Both models tend to overestimate measured values. A linear regression between models #4 and #5 showed an R^2 of 0.68. The model that used predicted WSA was more accurate at 300°C than at 100°C probably because there were no differences between unheated soils and 100°C. However, the model that used measured WSA was more relevant at 100°C. Despite this, at 300°C, the changes in WSA were significant, making the measured data less accurate for the model. These results show that a reliable WSA prediction is more difficult as the heating temperature increases. These can be attributed to the carbonization of soil, where OM content and clay decreased significantly.

This study focused on two specific temperatures (100 and 300°C), which may not fully capture all the possible effects observed in natural burnt or heated soils. Fire may increase or decrease aggregate stability, and in some cases, both effects can occur within the same soil affected by fire, depending on the severity gradient (Thomaz, 2021). Given this complexity, laboratory experiments are crucial for maintaining a constant temperature over a set period and minimizing spatial variability in results. Such controlled conditions allow a better understanding of how soils affected by fire interact with their environment (Martínez *et al.*, 2022). However, despite these controlled conditions, Varela *et al.* (2015) found that the effects of heating on water-stable aggregates (WSA) in laboratory experiments were comparable to those observed in naturally burnt soils, suggesting that laboratory experiments can effectively simulate wildfire impacts.

High-severity burn temperatures (>300°C) may also induce critical changes on soil water-stable aggregates, but these were not tested. On the other hand, the pedotransfer functions were developed based on soils with specific properties (texture, OM content, bulk density, and pH). Their applicability to other fire or heating regimes and inorganic cementing agents should be explored and validated with additional data. The study captures immediate post-heating changes but does not account for long-term recovery processes such as organic matter and mineral transformation.

4. CONCLUSIONS

This study provides a series of models to predict the effect of heating on the water stable aggregate (WSA) using variables typically measured in soil analysis routines. Overall, the soil properties selected in this study did not change significantly when the soils were exposed to 100°C. However, when heated at 300°C, organic matter (OM) and clay contents decreased significantly while the pH increased. These changes highlight the difference or lack of correlation between unheated soils and those exposed at 300°C, demonstrating that some soil properties are highly sensitive to high temperatures. The WSA decreased with heating, particularly at 300°C. This indicates that soil properties, such as soil quality or soil health, can be highly affected by heating due to aggregate breakdown.

Using basic or typical soil measurements proved to be useful for creating simple models to predict WSA in unheated soils and at 100°C. These models are an alternative when reducing the amount of extended laboratory experiments or field campaigns. After comparing the model developed by Rivera and Bonilla (2020) to an equivalent non-linear new model, this last one showed a better fit and accuracy, and it can be used as an alternative to predict WSA in unheated soils. On the other hand, four different models were developed for predicting the effect of heating on the WSA using basic properties from unheated soils, either using measured or predicted WSA. These models to predict WSA in heated soils showed that the pH, OM, and clay contents were key variables when predicting the temperature effects. Using the WSA values in unheated soils when predicting the effect of the temperature varies depending on the temperature itself. Using the measured WSA in unheated soils (model #2) was better for predicting the WSA at 100°C. However, the predicted WSA in unheated soils (model #5) proved to be better for the estimates at 300°C.

Conflicts of interest: The authors declare that there are no conflicts of interest.

5. REFERENCES

Acevedo, S.E., Martínez, S.I., Contreras, C.P., and Bonilla, C.A., 2023. Effect of data availability and pedotransfer estimates on water flow modelling in wildfire-affected soils. J. Hydrol. 617, 128919. https://doi.org/10.1016/j.jhydrol.2022.128919

Acevedo, S.E., Rivera, J.I., Acuña, E., Contreras, C.P., Giraldo, C.V., Ávila, C.J., *et al*., 2021. Soil data management at laboratory scale focused on soil physical measurements. ASA, CSSA, SSSA International Annual Meeting, Salt Lake, UT. https://scisoc.confex.com/scisoc/2021am/prelim.cgi/Paper/138826

Aedo, S.A., Bonilla, C.A., 2021. A numerical model for linking soil organic matter decay and wildfire severity. Ecological Modelling, 447, 109506. https://doi.org/10.1016/j.ecolmodel.2021.109506

Agbeshie, A.A., Abugre, S., Atta-Darkwa.T., Awuah, R., 2022. A review of the effects of forest fire on soil properties. J. Forestry Res. 33(5), 1419-1441. https://doi.org/10.1007/s11676-022-01475-4

Albalasmeh, A.A., Berli, M., Shafer, D.S., Ghezzehei, T.A., 2013. Degradation of moist soil aggregates by rapid temperature rise under low intensity fire. Plant Soil 362(1), 335-344. https://doi.org/10.1007/s11104-012-1408-z

Archontoulis, S.V., and Miguez, F.E., 2015. Nonlinear regression models and applications in agricultural research. Agronomy J. 107(2), 786-798. https://doi.org/10.2134/agronj2012.0506

Ayoubi, S., Mirbagheri, Z., Mosaddeghi, M.R., 2020. Soil organic carbon physical fractions and aggregate stability influenced by land use in humid region of northern Iran. Int. Agrophys. 34(3), 343-353. https://doi.org/10.31545/intagr/125620

Ayoubi, S., Rabiee, S., Mosaddeghi, M.R., Abdi, M.R., Abbaszadeh Afshar, F., 2021. Soil erosion and properties as affected by fire and time after fire events in steep rangelands using 137Cs technique. Arabian J. Geosci. 14(2), 113. https://doi.org/10.1007/s12517-020-06351-1

Badía-Villas, D., González-Pérez, J.A., Aznar, J.M., Arjona-Gracia, B., Martí-Dalmau, C., 2014. Changes in water repellency, aggregation and organic matter of a mollic horizon burned in laboratory: Soil depth affected by fire. Geoderma 213, 400-407. https://doi.org/10.1016/j.geoderma.2013.08.038

Bai, Y., Zhou, Y., He, H., 2020. Effects of rehabilitation through afforestation on soil aggregate stability and aggregate-associated carbon after forest fires in subtropical China. Geoderma 376, 114548. https://doi.org/10.1016/j.geoderma.2020.114548

Bonilla, C.A., Johnson, O.I., 2012. Soil erodibility mapping and its correlation with soil properties in Central Chile. Geoderma 189-190, 116-123. https://doi.org/10.1016/j.geoderma.2012.05.005

Bonilla, C.A., Pastén, P.A., Pizarro, G.E., González, V.I., Carkovic, A.B., Céspedes, R.A., 2014. Forest Fires and Soil Erosion Effects on Soil Organic Carbon in the Serrano River Basin (Chilean Patagonia). In: A. E. Hartemink and K. McSweeney (Eds), Soil Carbon (pp. 229-237). Springer Int. Publ. https://doi.org/10.1007/978-3-319-04084-4_24

Campo, J., Gimeno-García, E., Andreu, V., González-Pelayo, O., Rubio, J.L., 2014. Cementing agents involved in the macro- and microaggregation of a Mediterranean shrubland soil under laboratory heating. Catena 113, 165-176. https://doi.org/10.1016/j.catena.2013.10.002

Carkovic, A.B., Pastén, P.A., Bonilla, C.A., 2015. Sediment composition for the assessment of water erosion and nonpoint source pollution in natural and fire-affected landscapes. Sci. Total Environ. 512-513, 26-35.

Natural Resources Information Center, 1996a. Soil Survey – Metropolitan Region. Soil description, materials, and symbols. https://biblioteca.inia.cl/handle/20.500.14001/55234

Natural Resources Information Center, 1996b. Soil Survey - VI Region. Soil description, materials, and symbols. Pub. CIREN N°114. CIREN. https://bibliotecadigital.ciren.cl/handle/20.500.13082/13635

Natural Resources Information Center, 1997a. Soil Survey - V Region. Soil description, materials, and symbols. Pub. CIREN N°116. CIREN. https://bibliotecadigital.ciren.cl/handle/20.500.13082/24688

Natural Resources Information Center, 1997b. Soil Survey - VII Region. Soil description. https://bibliotecadigital.ciren.cl/handle/20.500.13082/2276

Natural Resources Information Center, 2002. Soil Survey - IX Region. Soil description, materials, and symbols. CIREN. https://bibliotecadigital.ciren.cl/handle/20.500.13082/24409

Chicco, J. M., Mandrone, G., Vacha, D., 2023. Effects of wildfire on soils: Field studies and modelling on induced underground temperature variations. Frontiers Earth Sci. 11, 1307569. https://doi.org/10.3389/feart.2023.1307569

Clergue, T.C., Saby, N.P. A., Wadoux, A.M.J.-C., Barthès, B.G., Lacoste, M., 2023. Estimating soil aggregate stability with infrared spectroscopy and pedotransfer functions. Soil Security 11, 100088. https://doi.org/10.1016/j.soisec.2023.100088

Contreras, C.P., Bonilla, C.A., 2018. A comprehensive evaluation of pedotransfer functions for predicting soil water content in environmental modeling and ecosystem management. Sci. Total Environ. 644, 1580-1590. https://doi.org/10.1016/j.scitotenv.2018.07.063

Corporación Nacional Forestal., 2024. Estadísticas – Resumen Regional Ocurrencia (Número) y Daño (Superficie Afectada) por Incendios Forestales 1977-2023. Estadísticas Históricas. https://www.conaf.cl/incendios-forestales/incendios-forestales-en-chile/estadisticas-historicas/

Dhungana, B.P., Thapa Chhetri, V., Baniya, C.B., Sharma, S.P., 2024. Low-intensity wildfire alters selected soil properties in the tropical shorea robusta forest. Int. J. Forestry Res. 1-11. https://doi.org/10.1155/2024/4686760

Durner, W., Iden, S.C., von Unold, G., 2017. The integral suspension pressure method (ISP) for precise particle-size analysis by gravitational sedimentation. Water Res. Res. 53(1), 33-48. https://doi.org/10.1002/2016WR019830

Farid, A., Alam, M.K., Goli, V.S.N.S., Akin, I.D., Akinleye, T., Chen, X., *et al*., 2024. A review of the occurrence and causes for wildfires and their Impacts on the geoenvironment. Fire 7(8), 295. https://doi.org/10.3390/fire7080295

Fox, D.M., Darboux, F., Carrega, P., 2007. Effects of fire-induced water repellency on soil aggregate stability, splash erosion, and saturated hydraulic conductivity for different size fractions. Hydrological Processes 21(17), 2377-2384. https://doi.org/10.1002/hyp.6758

Giraldo, C.V., Acevedo, S.E., Contreras, C.P., Santibáñez, F., Sáez, E., Calderón, F.J., *et al*., 2024. Effects of soil heating changes on soil hydraulic properties in Central Chile. Geoderma 449, 117013. https://doi.org/10.1016/j.geoderma.2024.117013

Groemping, U., 2007. Relative importance for linear regression in R: The Package relaimpo. J. Statistical Software 17, 1-27. https://doi.org/10.18637/jss.v017.i01

Hrelja, I., Šestak, I., Bogunović, I., 2020. Wildfire impacts on soil physical and chemical properties – A short review of recent studies. Agric. Conspectus Scientificus, 85(4), Article 4.

Ibrahimi, K., Mowrer, J., Amami, R., Belaid, A., 2019. Burn effects on soil aggregate stability and water repellency of two soil types from East and North Tunisia. Communications Soil Sci. Plant Analysis 50(7), 827-837. https://doi.org/10.1080/00103624.2019.1589487

Inbar, A., Lado, M., Sternberg, M., Tenau, H., Ben-Hur, M., 2014. Forest fire effects on soil chemical and physicochemical properties, infiltration, runoff, and erosion in a semiarid Mediterranean region. Geoderma 221-222, 131-138. https://doi.org/10.1016/j.geoderma.2014.01.015

Jiménez-Pinilla, P., Mataix-Solera, J., Arcenegui, V., Delgado, R., Martín-García, J.M., Lozano, E., *et al*., 2016. Advances in the knowledge of how heating can affect aggregate stability in Mediterranean soils: A XDR and SEM-EDX approach. Catena 147, 315-324. https://doi.org/10.1016/j.catena.2016.07.036

Khaledian, Y., Brevik, E.C., Pereira, P., Cerdà, A., Fattah, M.A., Tazikeh, H., 2017. Modeling soil cation exchange capacity in multiple countries. Catena 158, 194-200. https://doi.org/10.1016/j.catena.2017.07.002

Köster, K., Aaltonen, H., Berninger, F., Heinonsalo, J., Köster, E., Ribeiro-Kumara, C., Sun, H., *et al*., 2021. Impacts of wildfire on soil microbiome in Boreal environments. Current Opinion in Environ. Sci. Health 22, 100258. https://doi.org/10.1016/j.coesh.2021.100258

Li, T., Jeřábek, J., Winkler, J., Vaverková, M.D., Zumr, D., 2022. Effects of prescribed fire on topsoil properties: A small-scale straw burning experiment. J. Hydrol. Hydromechanics, 70(4), 450-461.

Marcos, E., Tárrega, R., Luis, E., 2007. Changes in a Humic Cambisol heated (100-500°C) under laboratory conditions: The significance of heating time. Geoderma 138(3), 237-243. https://doi.org/10.1016/j.geoderma.2006.11.017

Marcos, E., Fernández-García, V., Fernández-Manso, A., Quintano, C., Valbuena, L., Tárrega, R., *et al*., 2018. Evaluation of composite burn index and land surface temperature for assessing soil burn severity in Mediterranean fire-prone pine ecosystems. Forests 9(8), 494. https://doi.org/10.3390/f9080494

Martínez, S.I., Contreras, C.P., Acevedo, S.E., Bonilla, C.A., 2022. Unveiling soil temperature reached during a wildfire event using ex-post chemical and hydraulic soil analysis. Sci. Total Environ. 822, 153654. https://doi.org/10.1016/j.scitotenv.2022.153654

Mataix-Solera, J., Cerdà, A., Arcenegui, V., Jordán, A., Zavala, L.M., 2011. Fire effects on soil aggregation: A review. Earth-Science Rev. 109(1), 44-60. https://doi.org/10.1016/j.earscirev.2011.08.002

Meserve, P.L., Gómez-González, S., Kelt, D.A., 2020. The Chilean Matorral: Characteristics, Biogeography, and Disturbance. In M.I. Goldstein and D.A. DellaSala (Eds), Encyclopedia of the World's Biomes, Elsevier 594-601. https://doi.org/10.1016/B978-0-12-409548-9.11985-2

Molina-Roco, M., Escudey, M., Antilén, M., Arancibia-Miranda, N., Manquián-Cerda, K., 2018. Distribution of contaminant trace metals inadvertently provided by phosphorus fertilisers: Movement, chemical fractions and mass balances in contrasting acidic soils. Environ. Geochemistry Health 40(6), 2491-2509. https://doi.org/10.1007/s10653-018-0115-y

Negri, S., Arcenegui, V., Mataix-Solera, J., Bonifacio, E., 2024. Extreme water repellency and loss of aggregate stability in heat-affected soils around the globe: Driving factors and their relationships. Catena 244, 108257. https://doi.org/10.1016/j.catena.2024.108257

Negri, S., Stanchi, S., Celi, L., Bonifacio, E., 2021. Simulating wildfires with lab-heating experiments: Drivers and mechanisms of water repellency in alpine soils. Geoderma 402, 115357. https://doi.org/10.1016/j.geoderma.2021.115357

Ozlu, E., Arriaga, F.J., 2021. The role of carbon stabilization and minerals on soil aggregation in different ecosystems. Catena 202, 105303. https://doi.org/10.1016/j.catena.2021.105303

R Core Team, 2022. R: A language and environment for statistical computing (4.2.2) [Computer software]. R Foundation for Statistical Computing. https://www.R-project.org/

Ramírez, P.B., Calderón, F.J., Fonte, S.J., Santibáñez, F., Bonilla, C.A., 2020. Spectral responses to labile organic carbon fractions as useful soil quality indicators across a climatic gradient. Ecological Indicators 111, 106042. https://doi.org/10.1016/j.ecolind.2019.106042

Rieke, E.L., Bagnall, D.K., Morgan, C.L.S., Flynn, K.D., Howe, J.A., Greub, K.L.H., *et al*., 2022. Evaluation of aggregate stability methods for soil health. Geoderma 428, 116156. https://doi.org/10.1016/j.geoderma.2022.116156

Rivera, J.I., Bonilla, C.A., 2020. Predicting soil aggregate stability using readily available soil properties and machine learning techniques. Catena 187, 104408. https://doi.org/10.1016/j.catena.2019.104408

Roshan, A., Biswas, A., 2023. Fire-induced geochemical changes in soil: Implication for the element cycling. Sci. Total Environ. 868, 161714. https://doi.org/10.1016/j.scitotenv.2023.161714

Royal Eijkelkamp., 2022. Wet sieving apparatus for disturbed samples. Royal Eijkelkamp. https://www.royaleijkelkamp.com/products/soil-lab-testing-equipment/soil-physical-research/aggregate-stability/wet-sieving-apparatus/

Sadzawka R.A., Carrasco R.M.A., Grez Z.R., Mora G.M. de la Luiz, Flores P.H., Neaman, A., 2006. Recommended methods for soil analysis in Chile. 2006 Revision. https://biblioteca.inia.cl/handle/20.500.14001/8541

Sarricolea, P., Herrera-Ossandon, M., Meseguer-Ruiz, Ó. (2017). Climatic regionalisation of continental Chile. J. Maps 13(2), 66-73. https://doi.org/10.1080/17445647.2016.1259592

Soil Survey Staff., 2022. Kellogg soil survey laboratory methods manual, Part one: Current methods. Department of Agriculture, Natural Resources Conservation Service. https://www.nrcs.usda.gov/wps/portal/nrcs/detail/soils/ref/?cid=nrcs142p2_054247

Stavi, I., 2019. Wildfires in grasslands and shrublands: A Review of impacts on vegetation, soil, hydrology, and geomorphology. Water 11(5), 10-42. https://doi.org/10.3390/w11051042

Terefe, T., Mariscal-Sancho, I., Peregrina, F., Espejo, R., 2008. Influence of heating on various properties of six Mediterranean soils. A laboratory study. Geoderma 143(3), 273-280. https://doi.org/10.1016/j.geoderma.2007.11.018

Thomaz, E.L., 2021. Effects of fire on the aggregate stability of clayey soils: A meta-analysis. Earth-Science Reviews, 221, 103802. https://doi.org/10.1016/j.earscirev.2021.103802

Topa, D., Cara, I.G., Jităreanu, G., 2021. Long term impact of different tillage systems on carbon pools and stocks, soil bulk density, aggregation and nutrients: A field meta-analysis. Catena 199, 105102. https://doi.org/10.1016/j.catena.2020.105102

Valle, S.R., Dörner, J., Zúñiga, F., Dec, D., 2018. Seasonal dynamics of the physical quality of volcanic ash soils under different land uses in southern Chile. Soil Till. Res. 182, 25-34. https://doi.org/10.1016/j.still.2018.04.018

Varela, M.E., Benito, E., Keizer, J.J., 2015. Influence of wildfire severity on soil physical degradation in two pine forest stands of NW Spain. Catena 133, 342-348. https://doi.org/10.1016/j.catena.2015.06.004

Walkley, A., Black, I.A., 1934. An examination of the Degtjareff method for determining soil organic matter, and a proposed modification of the chromic acid titration method. Soil Sci. 37(1), 29.

Wei, T., Simko, V., 2024. R package “corrplot”: Visualization of a correlation matrix (Version 0.95) [Computer software]. https://github.com/taiyun/corrplot

Wickham, H., 2016. ggplot2: Elegant graphics for data analysis (3.4.0) [Computer software]. Springer-Verlag. https://ggplot2.tidyverse.org

Wickham, H., Averick, M., Bryan, J., Chang, W., McGowan, L.D., François, R., *et al*., 2019. Welcome to the tidyverse. J. Open Source Software, 4(43), 1686. https://doi.org/10.21105/joss.01686

Ye-Yang Chun, Liu, Z.-H., Zhou, D., Wu, C., Su, J., Luo, X.-Y., 2021. Effect of high temperatures (100-600°C) on the soil particle composition and its micro-mechanisms. Eurasian Soil Sci. 54(10), 1599-1607. https://doi.org/10.1134/S1064229321100045

Zavala L.M., Granged, A.J.P., Jordán, A., Bárcenas-Moreno, G., 2010. Effect of burning temperature on water repellency and aggregate stability in forest soils under laboratory conditions. Geoderma 158(3), 366-374. https://doi.org/10.1016/j.geoderma.2010.06.004

Zhang, F., Kong, R., Peng, J., 2018. Effects of heating on compositional, structural, and physicochemical properties of loess under laboratory conditions. Appl. Clay Sci. 152, 259-266. https://doi.org/10.1016/j.clay.2017.11.022